UNIVERSITY OF LEICESTER

SCHOOL OF ENGINEERING

Urban Air Mobility: Conceptual Design of a Novel Inter-city e-VTOL Aircraft and Its Integration with Existing Infrastructure

Module code:	**EG7020**
Module name:	**MSc Individual Project**

Date of submission: 10/10/2022

Author(s):	**Shreyash Kailas Hoval**
Student ID(s):	**219029097**
Degree:	**MSc Aerospace Engineering**
Tutor/Project supervisor:	**Dr. Paul Lefley**

SUPERVISOR'S COPY/EXAMINER'S COPY [For 3rd/4th year projects only - delete as appropriate]

I am aware of the University of Leicester's policy on plagiarism, and have taken the online tutorial on avoiding plagiarism. I am aware that plagiarism in this project report may result in the application of severe penalties up to and including expulsion from the University without a degree.

Summary

In recent years, there have been abundant innovative e-VTOL aircraft designs being developed for Urban Air Mobility. Although said to be market ready in upcoming few years, the concept of Urban Air Mobility is still quite open ended, therefore requires thorough investigations and scrutiny. This project explores the concept of UAM and introduces a novel e-VTOL conceptual vehicle called *Rhacophorus*. All stages of design methodology are appraised thoroughly while designing the aircraft with Computer Aided Design (CAD) software. Investigation of air flow behaviour is carried out with the help of Computational Fluid Dynamics (CFD) simulations. The simulation results of the aircraft model proved to be of satisfactory performance in aerodynamics.

Contents

1 Introduction

The adoption of hybrid-electric and all-electric powered motors in the automobile industry has propelled continuous and faster innovations and advancement in battery technology, and in turn, the improved energy storage capability has made possible the betterment of the performance of such automobile. The appeal and success of growing electrification in automobile sector did not fail to catch the attention of the aviation industry. Electrification of aircraft promises a sustainable aerial mobility system in urban setting. This emerging industry is dubbed as Urban Air Mobility, which includes a wide variety of aerial systems, however, the primary interests being e-VTOL (Electric Vertical Take-off and Landing) aircraft for the transportation of goods and people. And hence, the long fantasized flying car might just be around the corner.

1.1 Urban Air Mobility: Definition

The Urban Air Mobility (UAM) industry is inevitable to emerge in the market before the end of this decade. It promises sustainable, affordable, green, and safe addition and/or alternative for conventional transportation system and offers to perform transport, logistics, surveillance, and first-response missions. The term Urban Air Mobility itself is still quite ambiguous, whose definition is likely to evolve along with the industry. According to National Aeronautics and Space Administration (NASA) [1], UAM falls under the umbrella of a broader field known as Advanced Air Mobility (AAM) which encompasses wide variety of aviation technologies capable of revolutionizing the integration of air mobility in day-to-day life. Such technologies may include small drones, electric aircraft, autonomous/remotely controlled flight, automated air traffic management, etc.

Because of the ambiguity of the term, Urban Air Mobility, it is desirable to choose a definition that extends to become an all-inclusive derivation of the field in contrast to constraining it. According to Tojal et al. [2], while regarding the ground environment of the UAM airspace, it is counterproductive to confine the meaning of word “urban” describing only cities and suburbs in the given context. Assuming that air mobility is likely to expand into an interconnected network of air transportation, it is of more convenience to regard air mobility operations taking place above all infrastructure and people regardless of city, town, or village as UAM. And hence, Tojal et al. [2] proposed the following definition: “Urban Air Mobility is a transformational mobility concept for urban areas, making use of all types of manned and unmanned aerial systems to perform any type of missions operated in a very low level (VLL) airspace (below 1000ft above highest obstacle in populated environments) that aims to improve the welfare of individual and organizations.”

The three main defining characteristics of Urban Air Mobility system are the aircraft, the airspace, and the applications.

1.1.1 Aircraft

The conventional aircraft are characterized based on their wing configuration, namely, fixed wing configuration and rotary wing configuration. Rotary wing aircraft employ their main rotor to generate lift as well as thrust. Fixed wing aircraft utilize wings to generate lift, whereas the thrust is generated by separate engines. However, recent innovations in the Urban Air Mobility have

employed hybrid configurations and thrust vectoring features in order to create efficient vertical take-off and landing (VTOL) capabilities. Therefore, it is necessary to clarify the novel aircraft configuration characterization in an all-inclusive manner. For the VTOL capabilities, it is evident that all configurations employ rotor mechanism to generate lift, however, the actual distinctions appear during the cruise performance. Therefore, to classify different aircraft configurations, it is convenient to use the cruise lift mechanism as the identifier. Therefore, for UAM e-VTOL aircraft during cruise flight, the aircraft that employ rotor mechanism as the primary source of lift can be classified as rotary wing aircraft, similarly, the aircraft that employ fixed wings as the primary source of lift can be classified as fixed wing aircraft.

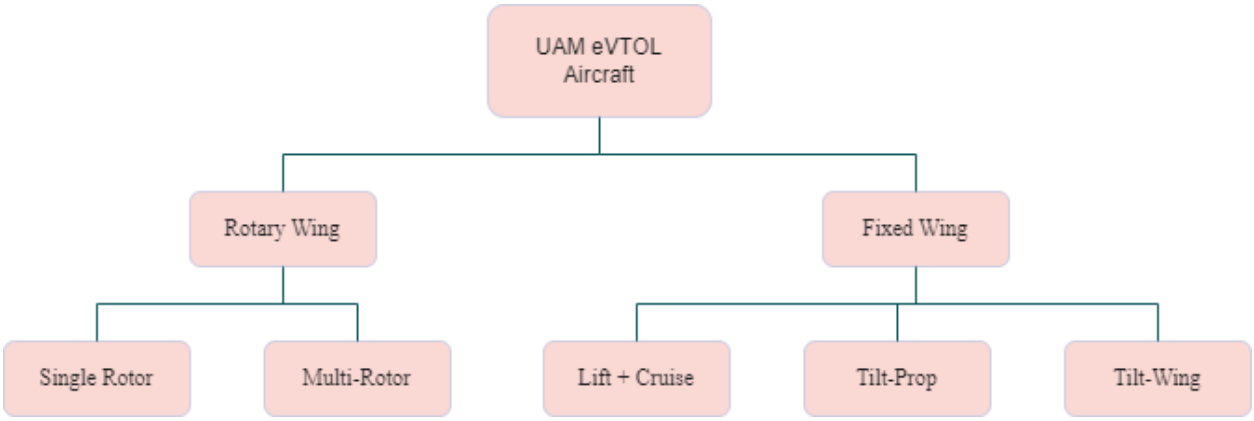

Figure 1 – e-VTOL Aircraft Configurations

A single rotor aircraft is identical to a conventional helicopter in terms of operation. However, in context of Urban Air Mobility, the rotor derives its power from an electric motor, instead of a turboshaft engine. The major advantage of this design is that it reduces the noise compared to the conventional helicopter. Also, the infrastructure required for this aircraft is already set in place.

Figure 2 – NASA Quiet Single Main Rotor Concept [3]

Multi-rotor configuration employs two or more rotors for vertical as well as horizontal flight. Rotation of rotor disc is employed for thrust vectoring. Most of the small drones in the market use quadrotor arrangement because of the proven reliability of the configuration.

NASA Side-by-Side Helicopter Concept [3]

NASA Quadcopter Concept [3]

EHang 184 [4]

Volocopter VoloCity [5]

Figure 3 – Different Multi-rotor Configurations

A lift + cruise (L + C) configuration aircraft has rotor arrangement for vertical and hover flight and has separate propellers for thrust generation in horizontal flight. This configuration may or may not utilize wings for lift generation.

Figure 4 – Volocopter VoloConnect Lift + Cruise Configuration [5]

The tilt wing configuration consists of multiple proprotors (act as propeller when horizontal and rotor when vertical) fixed on the wing. The wing is arranged to be able to tilt depending on the phase of the mission. The wing is positioned vertically during hover flight, whereas in cruise flight it is positioned horizontally and functions same as any conventional fixed wing aircraft to generate lift.

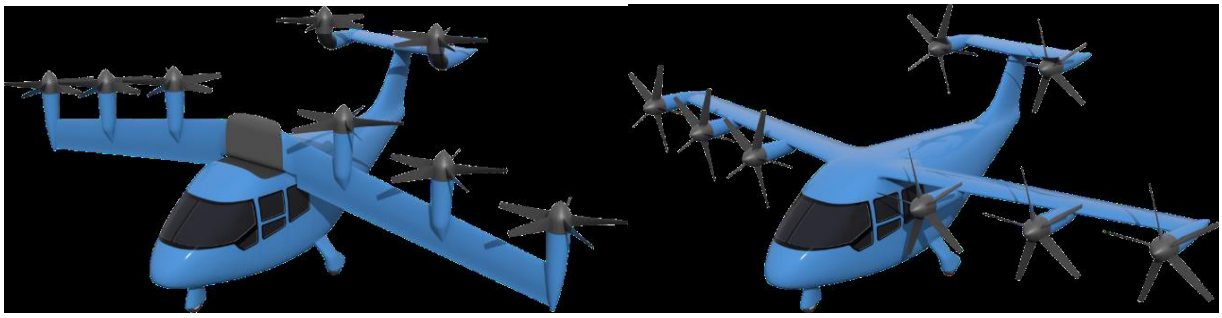

Hover Configuration Cruise Configuration

Figure 5 – NASA Tilt Wing Concept [6]

Tilt rotor configuration is not completely new to aviation, a popular example being the Bell Boeing V-22 Osprey. In UAM, the tilt rotor is an e-VTOL aircraft whose proprotors face vertically during hover and face horizontally during cruise flight.

Hover Configuration Cruise Configuration

Figure 6 – NASA Tilt Rotor Concept [7]

The first UAM vehicles to enter the market are envisioned to be either piloted or remotely piloted, and then a gradual transition to automated non-self-learning and automated self-learning UAS (Unmanned Aerial Systems).

1.1.2 Airspace

For the past few years, the emergence of Urban Air Mobility being in sight has pushed governments and local authorities to compile standardized rules, given the shear variety in which these aircraft come in. Additionally, the lower altitudes for operations, complexity of the environment of operation, the potential volume of operations and the widely varying performance range of aircraft have become biggest challenges compared to the traditional air traffic management. In Europe,

SESAR Joint Undertaking [8] is working on various projects in UAM, funded by the European Union. One of these projects is AMU-LED (Air Mobility Urban – Large Experimental Demonstrations) working on the capabilities of Unmanned Aircraft Systems Traffic Management (UTM), which is separate but complementary to the conventional Air Traffic Management (ATM). The airspace of UTM operations is dubbed as U-space [8], which is designed based on the envisioned UAM ecosystem and can accommodate the variety of aircraft and operations. The U-space is the airspace under VLL (below 1000ft above highest obstacle), the airspace higher than VLL is reserved for manned ATM. U-space is primarily divided into HPL (High Performance Layer) and SPL (Standard Performance Layer). AMU-LED agrees on the initial difficulties of coexistence of UTM and ATM, therefore the plan of action is to only utilize the altitude layer where manned air traffic is generally restricted. Therefore, the whole HPL is reserved for the aerial mobility of passengers and cargo for more efficient routes. Whereas the SPL will accommodate smaller UAVs (Unmanned Aerial Vehicles) with wide range of mission performances and safety implications.

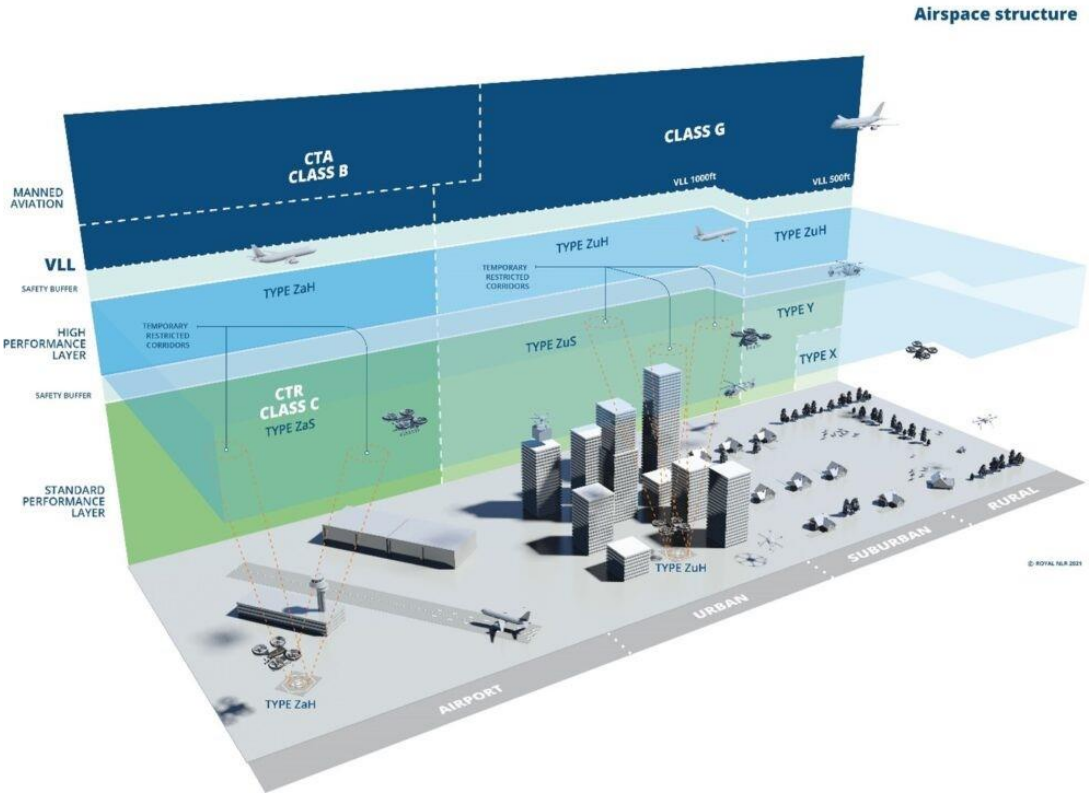

Figure 7 – AMU-LED Structure of UAM Airspace [9]

1.1.3 Applications

The fundamental drive behind the innovative designs for UAM aircraft is the enormous potential of wide variety of applications of this technology in the business world. To become successful in the business ecosystem, the Urban Air Mobility must overcome technological challenges such as battery technology, air traffic management, weather, and non-technological challenges such as public perception, laws and regulations, infrastructure, etc. However, with the new advancements in

battery technology and development of frameworks such as U-space, the trajectory of the industry points towards overcoming of most of the challenges in the near future. Therefore, it is important to carefully manage and regulate this mode of mobility from the beginning to allow its evolution into a sustainable and safe mode of transport. Hence, the governing bodies are not cutting corners for the new regulations before the eminent rise of UAM. To seize the potential market of UAM, the competition amongst the industry is palpable. Although the business applications of UAM are still under investigation, (Table 1) lists a modified version of [2]'s business applications for Urban Air Mobility with description and examples.

Table 1 – Business Applications of UAM [2]

Application		Description	Examples
Air Commute	**Shuttle Service**	Scheduled service along specified routes and at specified times	Airport shuttle, corporate shuttle
	Taxi Service	On-demand point-to-point passenger transportation	Air taxi
	Tourism	Scheduled or on-demand aerial sightseeing tours	Tourist shuttle
Air Ambulance		High-priority transport to and from hospitals Paramedic service to accident site	Air ambulance
Public Services	**First Response**	High-priority public services	Firefighters, natural disaster aid, police services
	Non-first Response	Day-to-day public services	Trash collection, hazardous waste disposal, snowplough, salt trucks
Surveillance		Real time video footage, pictures to provide surveillance capabilities for security and law enforcement	Police patrol, security, natural disaster aid
Scientific Research		Scientific data collected with drones for research purposes	Aerospace, environment, pollution, migration patterns
Delivery Service		Drones to deliver parcels or mail	Aerial warehousing, delivery of documents, delivery of goods
Point-to-Point Delivery Service		Shipment of heavy cargo between two locations	Heavy cargo delivery

High Priority Delivery	High-priority delivery equipment and goods	Humanitarian aid, high-priority medical delivery
Inspection	Use of drones for the inspection of urban infrastructure (e.g., roads, buildings vessels, power plants, etc.)	Infrastructure inspection, aerial warehousing
Utility Asset/Infrastructure Maintenance	Servicing and maintenance of utility assets and infrastructure	Servicing and maintenance of utility poles, live wires and maintenance of buildings or other infrastructure
Aerial Photography	Capturing video, pictures of objects, sites, people, etc.	Aerial filming, television, news reporting, recreational photography
Entertainment	Amusement Parks, extreme/adventure sports	Thrill rides, aerial acrobatics, parachuting platform
Construction and Real Estate	Construction of infrastructure and buildings, such as painting and window washing, to replace current access methods such as pulley platforms. Aerial showcasing, surveying, inspecting	Construction and maintenance of buildings and infrastructure Realtor showcasing buildings, house, or land to clients
Agriculture	Reaching less accessible areas for crop harvesting Remotely herding flocks Landscaping above ground, such as trees, cliffs	Harvesting, herding, landscaping

1.2 Project Aim and Objectives

The aim of this project is to explore the concept of Urban Air Mobility and to design a novel conceptual e-VTOL aircraft for intercity transportation of passengers or cargo. The design should be able to utilize aerodynamic characteristics of conventional aircraft combined with certain propulsion features of modern drones.

A conceptual design methodology suitable for e-VTOL UAM aircraft proposed by Palaia et al. [8] was chosen to design a novel e-VTOL concept aircraft called *Rhacophorus*. Derivation of appropriate

equations to clearly demonstrate design parameter. Design of detailed UAM mission definition. Use of SolidWorks software package to design a full-scaled model. To test the aerodynamic performance, ANSYS Fluent software was chosen to be used. The estimation of aerodynamic forces on the fuselage and wings will also be acquired from the ANSYS Fluent simulation results.

2 Method

2.1 Design Workflow

The design methodology proposed by Palaia et al. [10] sets aerodynamics, mission analysis, and propulsion sizing as the main aspects of an aircraft design at the conceptual stage. Since, this methodology was developed for the design of e-VTOL aircraft, the propulsion sizing is specially formulated for electric propulsion units.

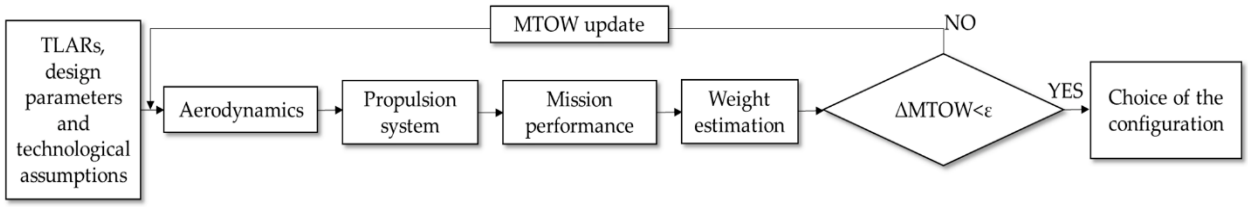

Figure 8 – Conceptual Design Workflow for UAM e-VTOLs [10]

The Top-Level Aircraft Requirements (TLARs) and design parameters are the primary design motivations that are dictated by the requirement specifications for the aircraft.

The aerodynamics section deals with the aerodynamic forces on the aircraft and their relation (drag polar) using Computational Fluid Dynamics.

The propulsion system is arranged based on the design's aerodynamic features and power requirements. The sizing of electric motors will be dealt in this section.

The mission performance section details the mission definition.

Finally, the weight of the aircraft will be estimated based on the design variables.

2.2 Design Parameters and TLARs

(a) Hover (b) Cruise

Figure 9 – Concept Design *Rhacophorus*

For most fixed wing e-VTOL configurations, the primary design parameters are wing loading $\frac{W}{S}$ and disc loading $\frac{T}{A}$ [10]. However, in these configurations, the during hover, the rotor discs alone counter the aircraft weight, and in cruise, the wings alone carry the aircraft weight.

The expressions [10] for wing loading and disc loading are,

$$\frac{W}{S} = \frac{W_{aircraft}}{S_{wing}} \qquad \text{(Equation 1)}$$

$$\frac{T}{A} = \frac{T_{propeller}}{A_{propeller}} \qquad \text{(Equation 2)}$$

Where, $W_{aircraft}$ is the weight of the aircraft, S_{wing} is the wing area, $T_{propeller}$ is the propeller thrust and $A_{propeller}$ is the propeller area.

Since, the *Rhacophorus* design is of a fixed-wing tilt prop quadrotor configuration (Figure 1), during hover, only the total disc loading on the quadrotor (2 rotors and 2 proprotors) counters the aircraft weight, whereas during cruise, the disc loading on 2 front rotors and the total wing loading counters the aircraft weight. Therefore, it is necessary to derive new set of equations that can fully demonstrate the primary performance parameter of the new aircraft.

Now, for the case of *Rhacophorus*, the expression of loading parameter in hover becomes,

$$X_{hover} = \frac{(T_{rotors}+T_{proprotors})}{(A_{rotors}+A_{proprotors})} = \frac{W_{aircraft}}{(A_{rotors}+A_{proprotors})} \qquad \text{(Equation 3)}$$

Where, X_{hover} is the loading parameter in hover, T_{rotors} is the total thrust force from two front rotors, $T_{proprotors}$ is the total thrust force from two rear proprotors, A_{rotors} is the total area of two front rotor discs, and $A_{proprotors}$ is the total area of the rear proprotor discs.

However, during lift-off, $W_{aircraft} < (T_{rotors} + T_{proprotors})$, and during landing, $W_{aircraft} > (T_{rotors} + T_{proprotors})$, therefore, the new expression for loading parameter in vertical flight becomes,

$$X_{vertical} = \frac{(T_{rotors}+T_{proprotors})}{(A_{rotors}+A_{proprotors})} \qquad \text{(Equation 4)}$$

Where, $X_{vertical}$ is the loading parameter in vertical flight.

Next, the expression for the loading parameter in cruise flight is,

$$X_{cruise} = \frac{L_{wings}}{S_{wings}} + \frac{T_{rotors}}{A_{rotors}} \qquad \text{(Equation 5)}$$

Where, X_{cruise} is the loading parameter, L_{wings} is the total lift force from both wings, and S_{wings} is the total wing area.

(Equations 3, 4, 5) fully express the loading parameter for *Rhacophorus* throughout the mission.

Table 2 – TLARs for UAM *Rhacophorus*.

Number of Passengers	7 to 8
Range	100 km
Cruise Speed (V_{cruise})	50 – 60 m/s
Cruise Altitude	300 m
Reserve Range	10 km

TLARs are the Top-Level Aircraft Requirements, which are dictated by the requirement specifications and designated mission profile for the e-VTOL UAM aircraft.

2.3 Design Evolution and Aerodynamics Methodology

This concept design was named *Rhacophorus* because of a slight resemblance to a flying frog species. The initial inspiration for the design of *Rhacophorus* was to modify and innovate the conventional quadcopter. The quadcopter relies solely on the four rotors for flight and does not accommodate any aerodynamic surfaces for the purpose of lift generation during flight. With the addition of passive aerodynamic surfaces (wings) for lift generation, the idea was to make a more efficient version of the quadcopter which does not solely rely on the four rotors for flight. Further, the inspiration for a combination of wings and rotor configuration with vectored thrust was drawn from the tilt-rotor Bell Boeing V-22 Osprey aircraft.

(a) Bell Boeing V-22 Osprey [11] (b) NASA Quadcopter Concept [3]

Figure 10 – Design Inspirations for the Concept

The idea was to combine certain design characteristics of a tilt rotor with the conventional quadcopter design. Various combinations of rotors and wing position were explored, In the end, finalizing the Figure 11(c) design.

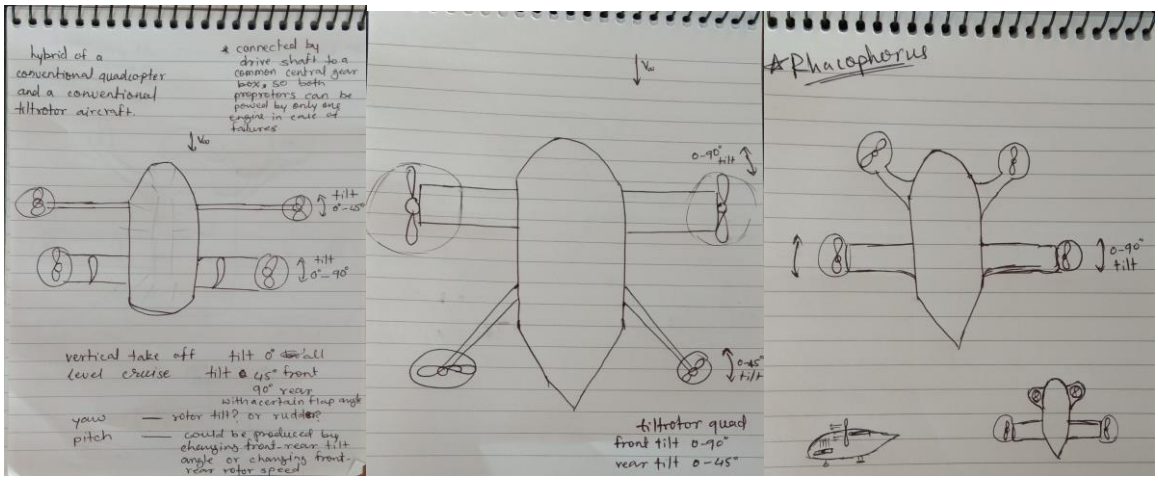

(a) (b) (c)

Figure 11 – Some Initial Rough Sketches of the Concept

The *Rhacophorus* design (Figure 9) employs the two front rotors as well as the rear proprotors for lift generation during take-off, hover, and landing. The rear wings and the two front rotors function as the primary sources of lift during cruise. The two proprotors mounted on the wings can tilt, and this gradual tilt, from facing upwards to facing forwards, is employed during the transition from take-off to climb to cruise for the horizontal component of the force required for forward flight. The proprotor tilt is employed again during the transition from cruise to descent to land. With help of appropriate calibration of flight control systems to balance the vertical components of forces from the wing and the front rotors, this aircraft will be airworthy. The *Rhacophorus* is designed to achieve a level-flight throughout the mission.

Manoeuvrability:

Yaw motion is achieved by vectoring the thrust from the front rotors sideways.

Roll motion can be achieved by manipulating power to the motors on either port or starboard side as desired.

Pitch motion can be achieved by manipulating power to the front rotors for create moment about the lateral axis.

Propeller ducts:

Propeller ducts are installed to increase the efficiency and the stability of the propeller. The ducts reduce power consumption as well as the noise and vibrations from the propeller. As the front rotors are closer to the fuselage, use of ducts can be advantageous. However, if ducts added to the rear proprotors, they will not be able to tilt because of the added stability effect from the ducts. Additionally, installing ducts on the rear proprotors can make the tilting mechanism and the manufacturing more complex.

2.3.1 CAD in SolidWorks Software

A three-view rough sketch was drawn as a reference for the SolidWorks sketch.

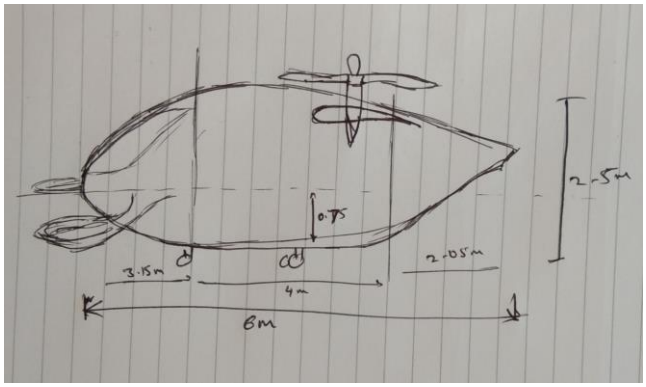

(a) Side View

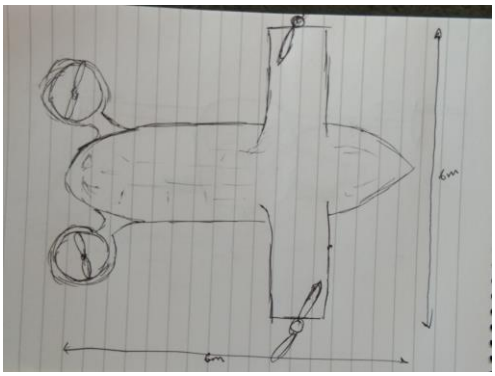

(b) Top View

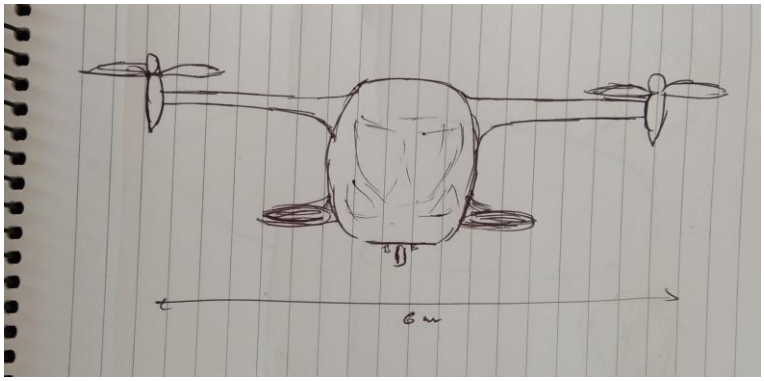

(c) Front View

Figure 12 – Initial Rough Sketch of the finalized Concept Design *Rhacophorus*

The Fuselage:

To design the fuselage part in SolidWorks, the side and top profiles were sketched and then pierced with closed spline at multiple key locations to create the enclosure profile. Because of the upward curvature of the empennage section from the side profile, the consistency of the enclosure started distorting. Therefore, manual calculations were employed to work out the geometry to trace the upward curvature of the side profile for the empennage section.

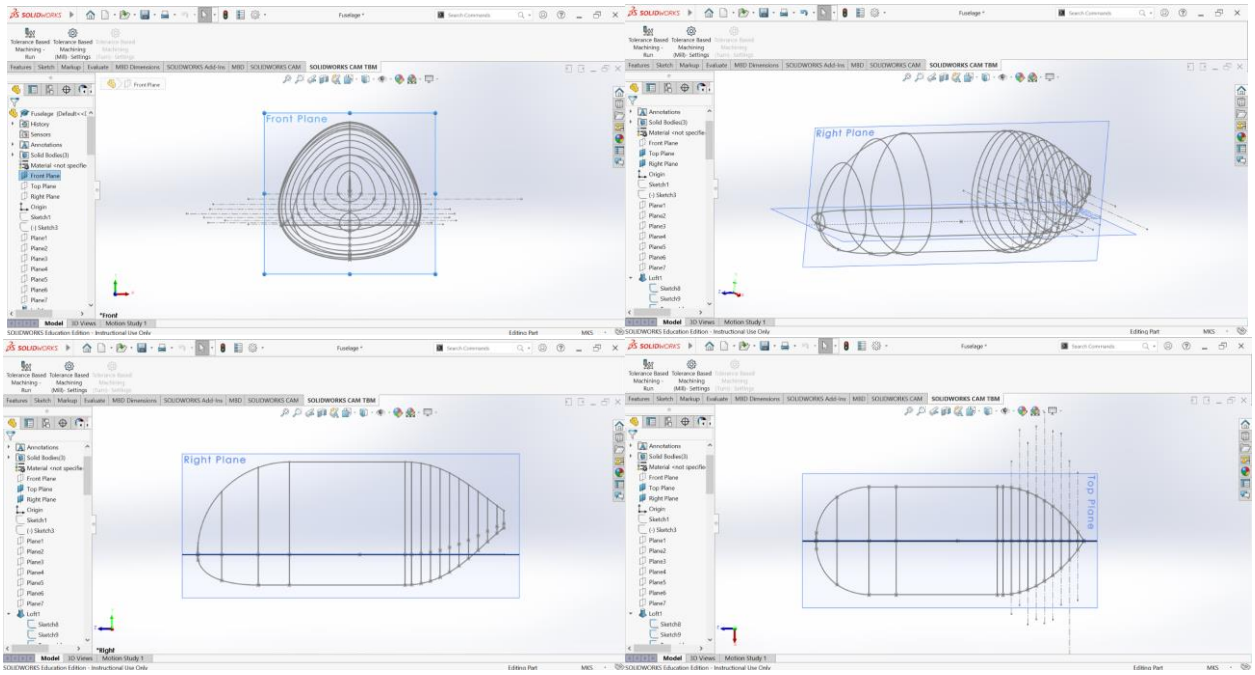

Figure 13 – 3D Computer Aided Fuselage Sketch - Iteration 1

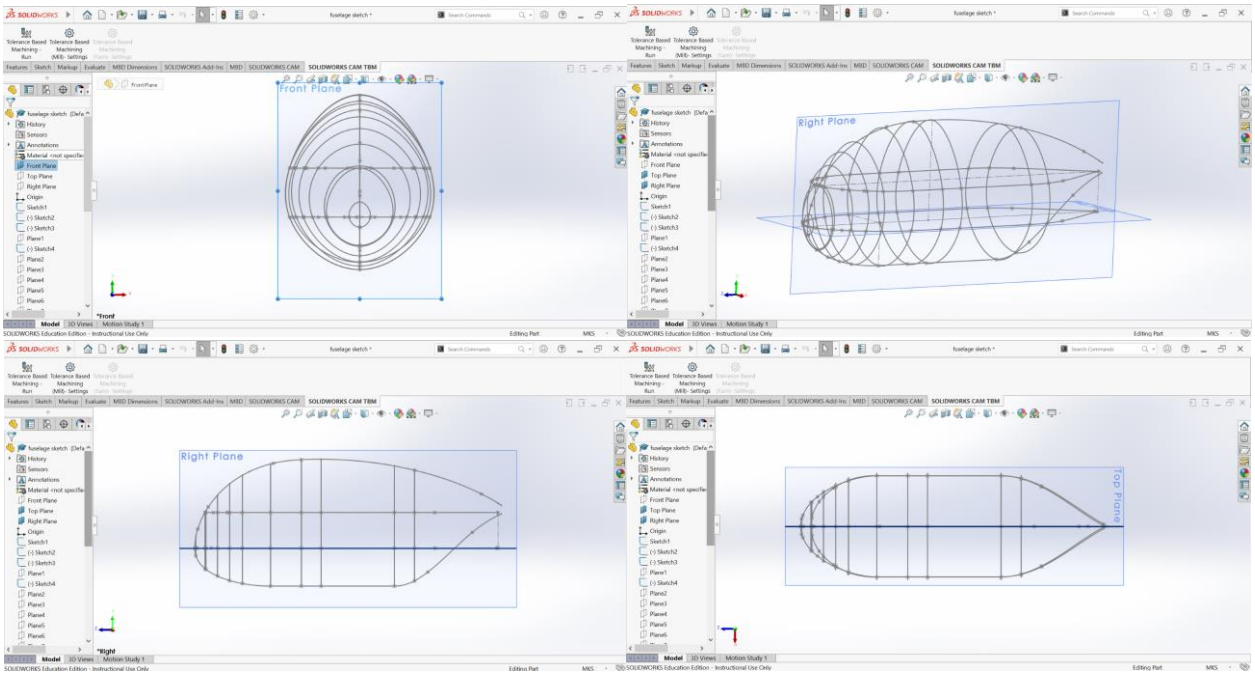

Figure 14 – 3D Computer Aided Fuselage Sketch - Iteration 2

Having a single horizontal top profile guide curve made the resulting fuselage side profile shape too curvy. Therefore, a trial-and-error method was used by adding more top profile guide curves in later iterations (see top view and side view - Figures 13, 14, 15, 17). Adding a second top profile guide curve did not improve the resulting shape (Figure 14) as desired, therefore a total of four horizontal top profile guide curves were layered which resulted in a satisfactory fuselage side profile shape in the iteration 3 (Figure 15).

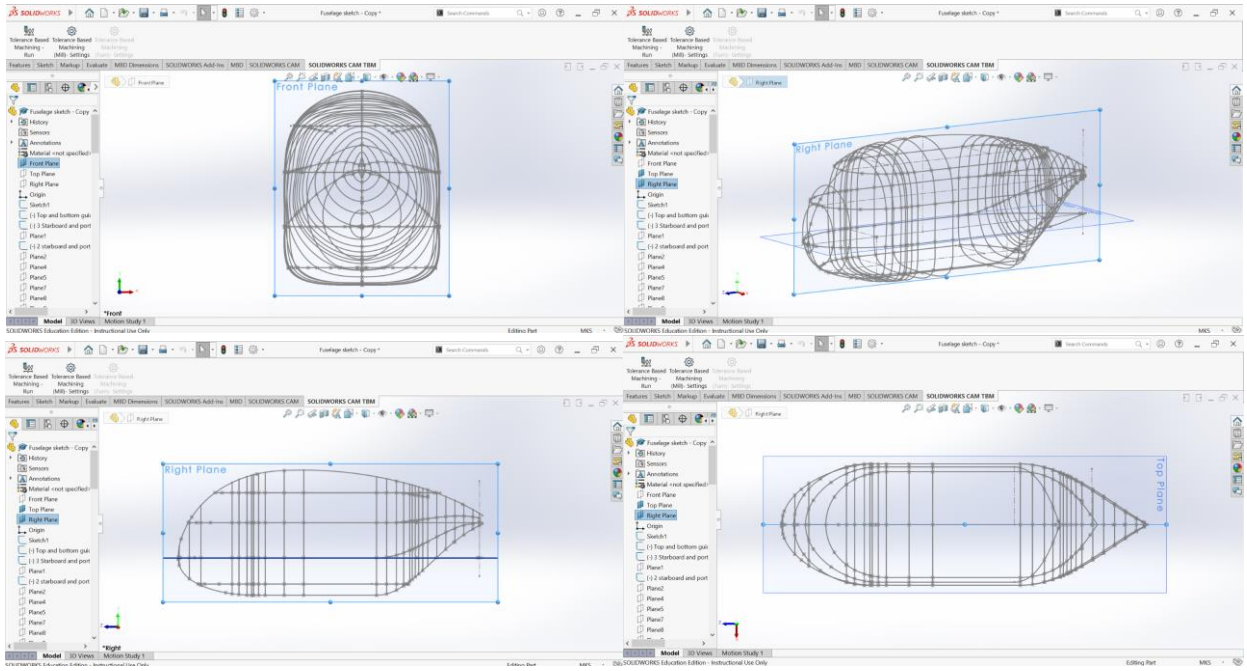

Figure 15 – 3D Computer Aided Fuselage Sketch - Iteration 3

The iteration 3 design was tested in computational fluid dynamics which resulted in undesirable behaviour of flow at the lower part of the empennage, therefore, the vertical side guide curve was altered (see side view – Figures 15, 16, 17) in iteration 4 to make the profile more aerodynamic and allow the flow to remain attached the lower part of empennage. The curvature comb function (Figure 16) of spline tool in SolidWorks proved to be reliable indication on aerodynamic smoothness of the profile. This led to desired results in ANSYS Fluent fluid flow study and the turbulent flow was reduced substantially.

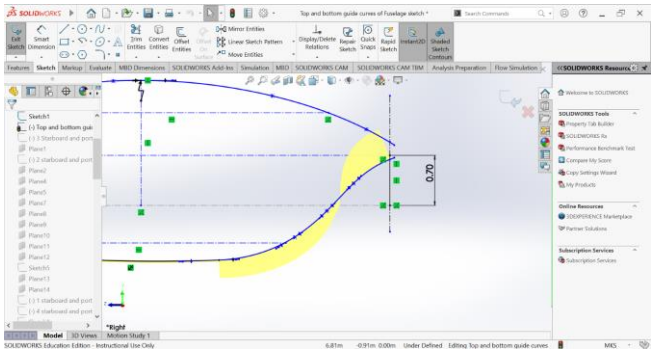

Figure 16 – New Side Guide Curve Curvature Comb for Empennage

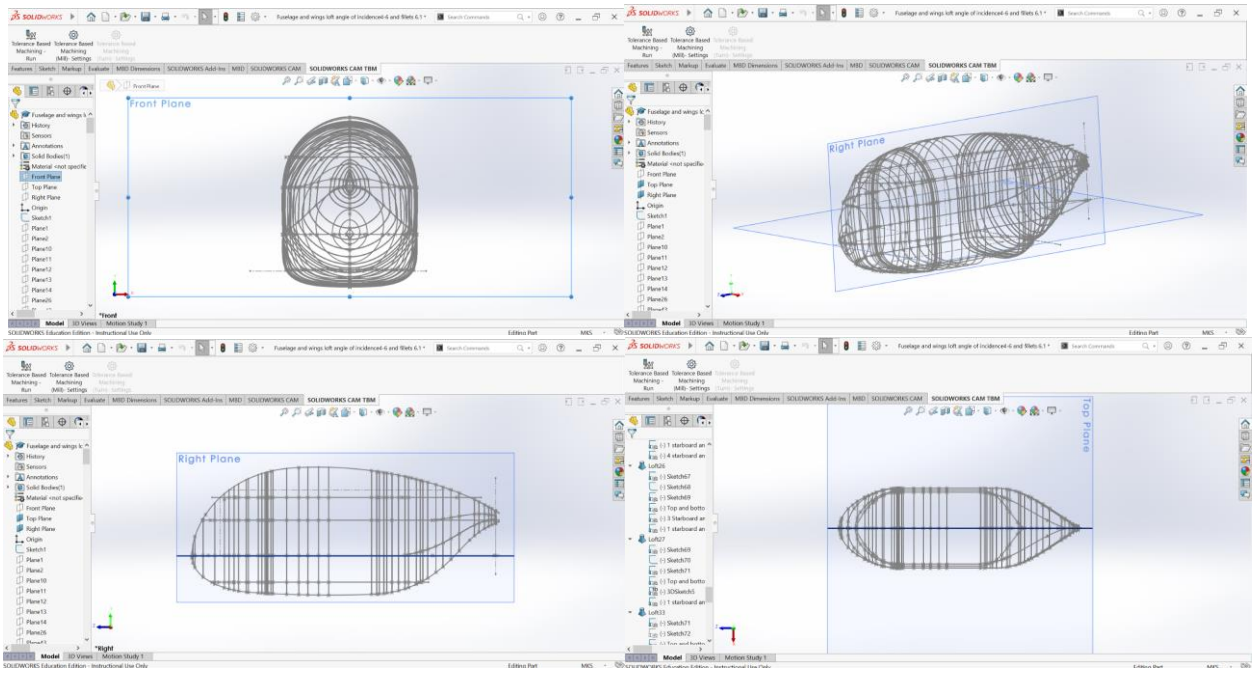

Figure 17 – 3D Computer Aided Fuselage Sketch - Iteration 4

Wings:

Since the *Rhacophorus* was designed for a level flight, the wings were placed at an 'angle of incidence' with the fuselage. The angle of incidence is the angle of cord line of the wing with the longitudinal axis. However, the angle of incidence is varied from the wing root to wing tip. This variation is called 'washout,' this is done to improve stalling characteristics. The angle of incidence for the rear wing were selected to be 6 degrees at wing-root and 4 degrees at wingtip. And for the front wing, 5 degrees at the wing-root and 4 degrees at the wingtip (Figure 19).

Since in this case, the longitudinal axis is horizontal, the angle of incidence is equal to the angle of attack (AoA). Hence, by comparing different NACA four-digit series airfoils [12], NACA2412 airfoil was found to be suitable. At velocities 50 m/s and 55 m/s, for the NACA2412 airfoil the aerodynamic efficiency factor $\left(\frac{C_l}{C_d}\right)$ was highest between angles of attack 4 degrees and 7 degrees (Figure 18). These results were obtained from ANSYS Fluent by simulating flow over NACA2412 airfoil.

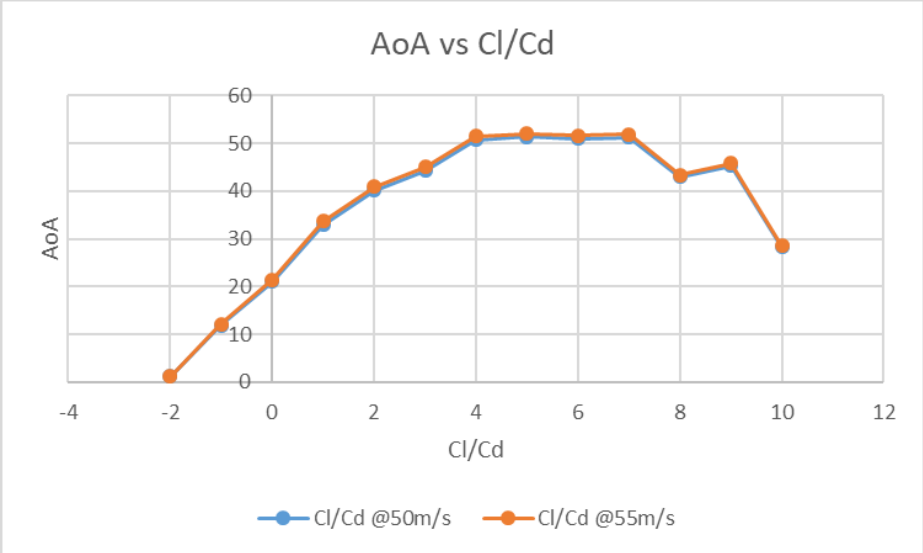

Figure 18 – NACA2412 AoA vs Aerodynamic Efficiency Factor

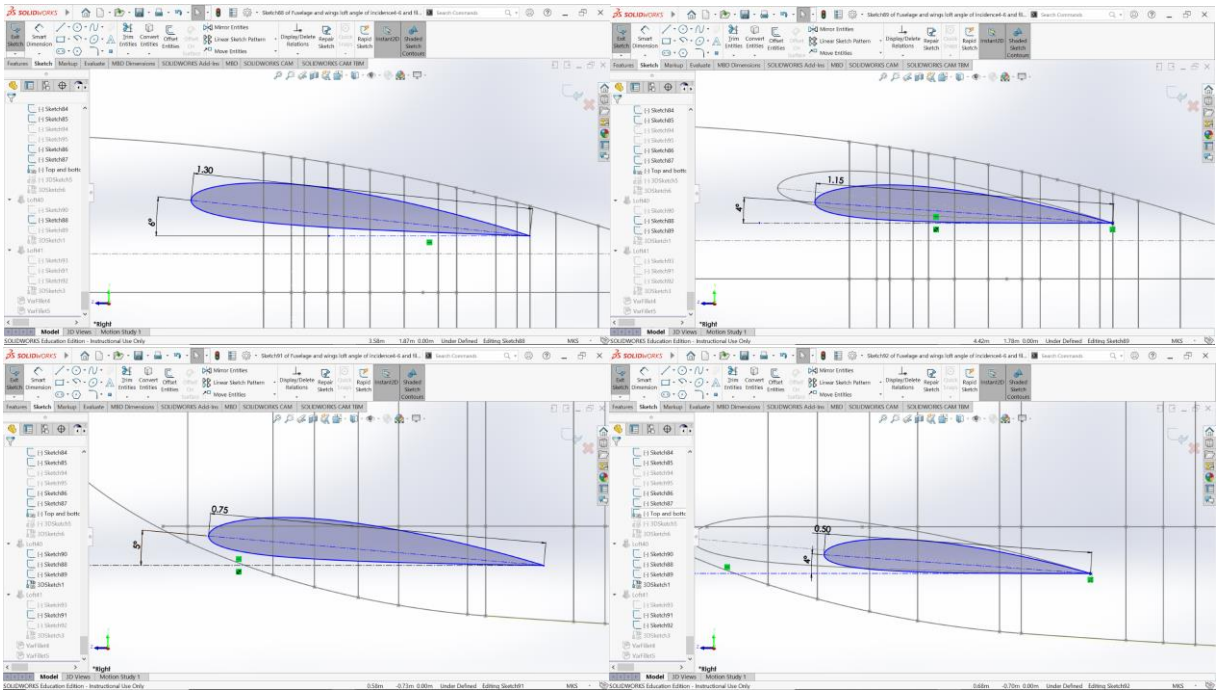

Figure 19 – Wing-root (left) and Wingtip (right) Sketches for the Rear and Front Wing

Loft:

The lofting tool from SolidWorks was used to complete the body of the fuselage and the wings. For smoother finish on the surface multiple sketch profiles were added on the guide curves (Figure 17) for the fuselage.

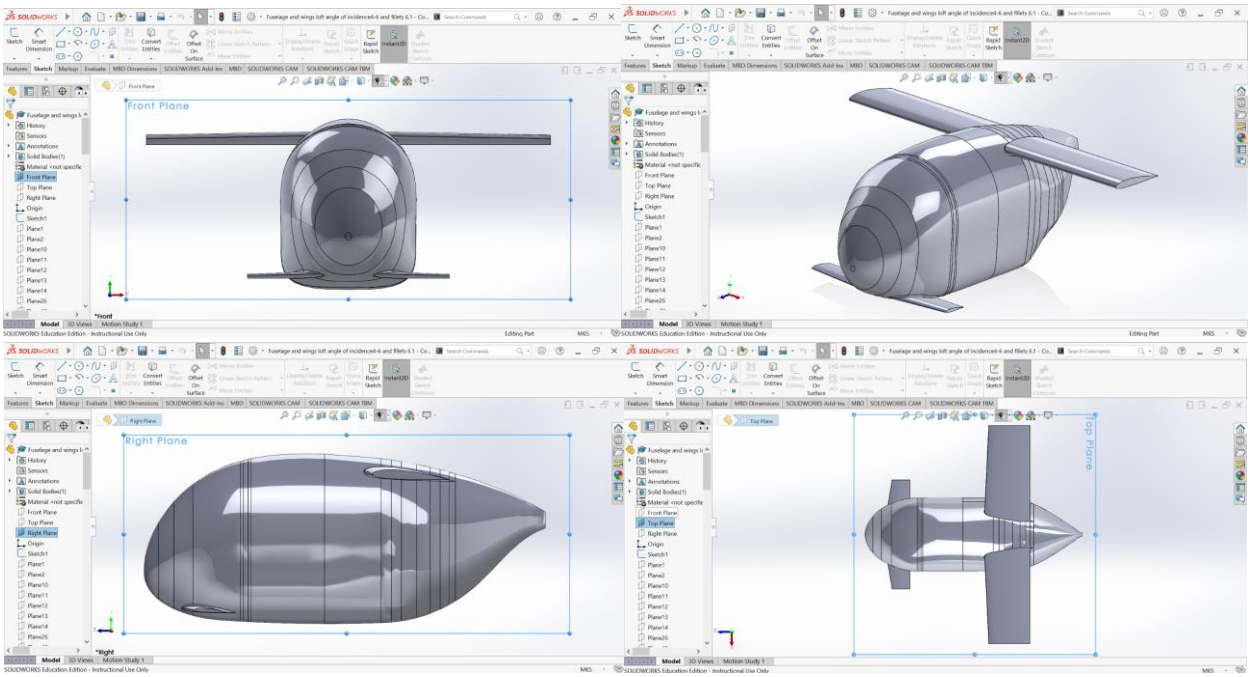

Figure 20 – Loft of the Fuselage and Wings

The proprotors, proprotor boss, rotor boss, etc. were also designed on SolidWorks using loft and extrude tools. All these parts were assembled on the software resulting in this (Figure 21, 22) final model. The proprotor boss was given a 90° angle freedom of movement to model both hover configuration (Figure 21) and cruise configuration (Figure 22).

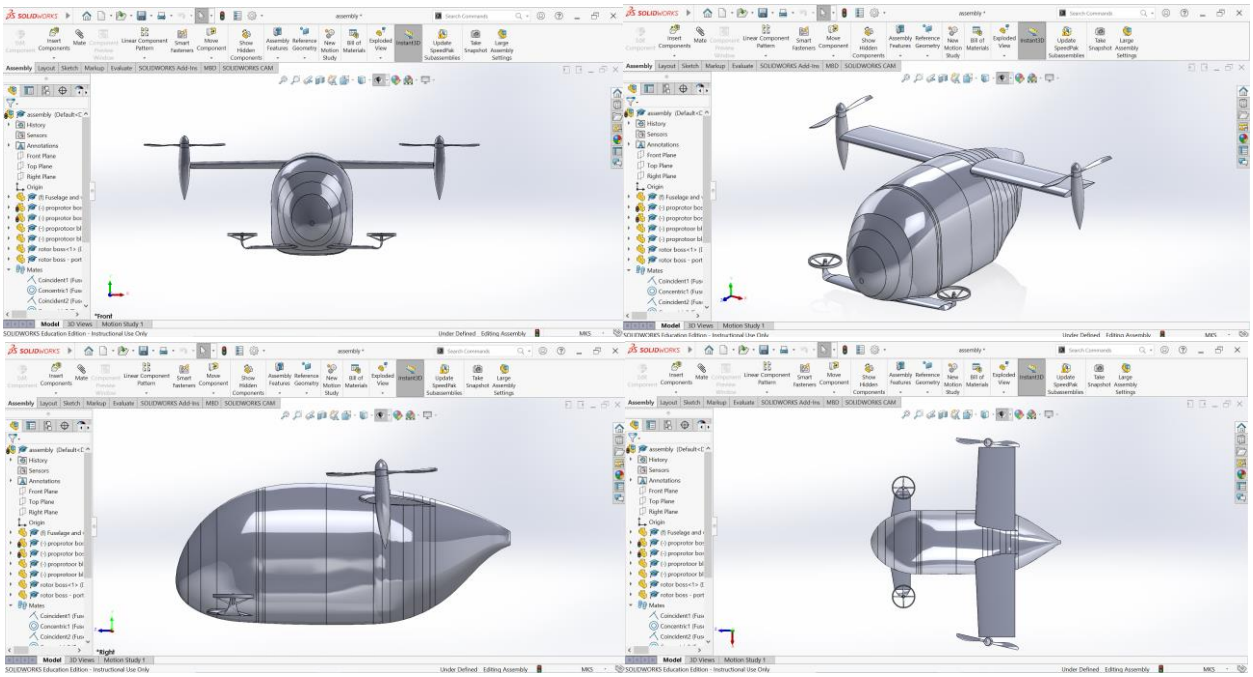

Figure 21 – Finished Model in Hover Configuration

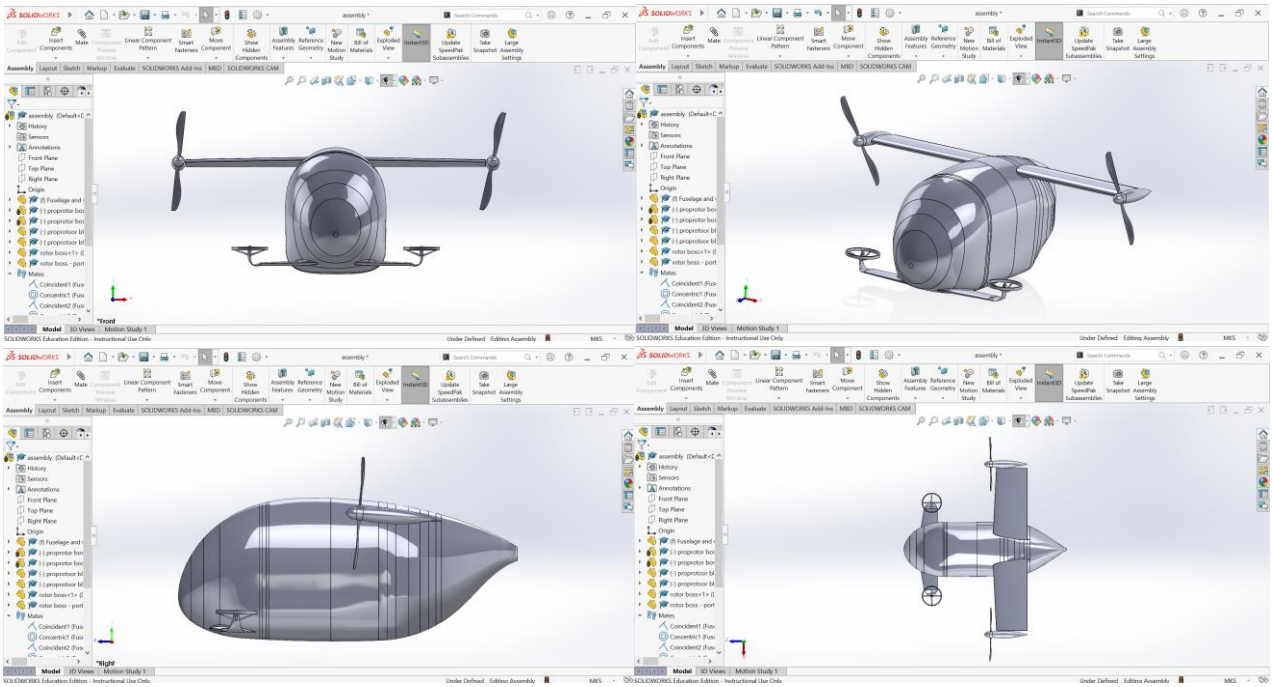

Figure 22 – Finished Model in Cruise Configuration

2.3.2 CFD Simulations in ANSYS Workbench

NACA2412 Airfoil:

Coordinates for NACA2412 airfoil were imported from [12]. The simulation of flow over airfoil NACA2412 was carried out in ANSYS Fluent to obtain the variation in aerodynamic efficiency with angle of attack (Figure 18). As the airfoil was chosen as the wing cross section, further simulations were run to obtain pressure and velocity variations because of flow behaviour. A highly dense triangular element mesh (Figure 23) was created with 45260 nodes and 89120 elements. The selected boundary conditions were no-slip. The viscous model selected for the simulation was k-omega, which is a 2-equation model and gives the best results for a 2D flow with high Reynold's number.

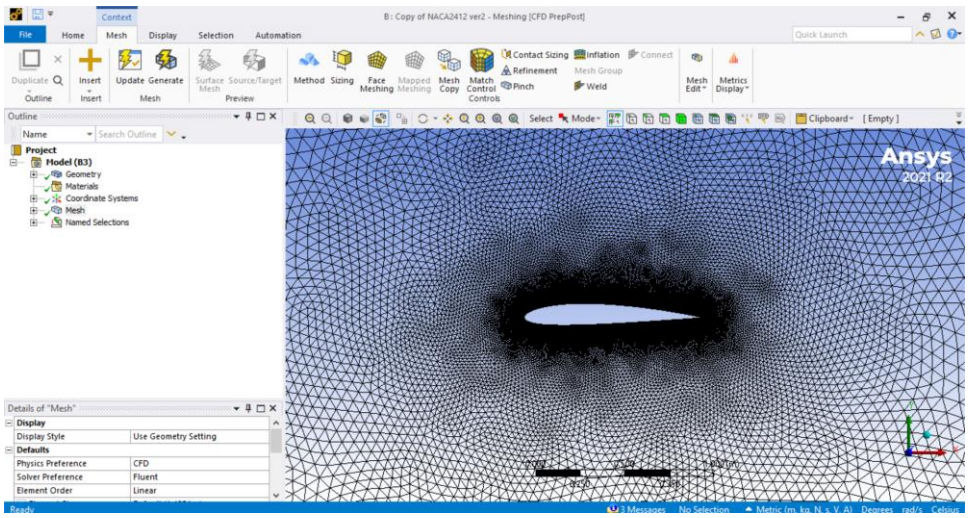

Figure 23 – NACA2412 Mesh

***Rhacophorus* Aircraft (Fuselage and Wings):**

The full-scale aircraft model was imported from SolidWorks to ANSYS Workbench to study the air flow over the surface in a 3D simulation. A highly dense tetrahedron mesh was created, having 336157 nodes and 1804085 elements. No-slip boundary conditions were selected on the aircraft surface, and specified shear boundary conditions were selected for the enclosure wall. The Realizable K-epsilon viscous model was selected. This viscous model also solves with two equations and provides comparatively accurate results for high Reynold's number flow and accurately represents the generation of turbulent kinetic energy.

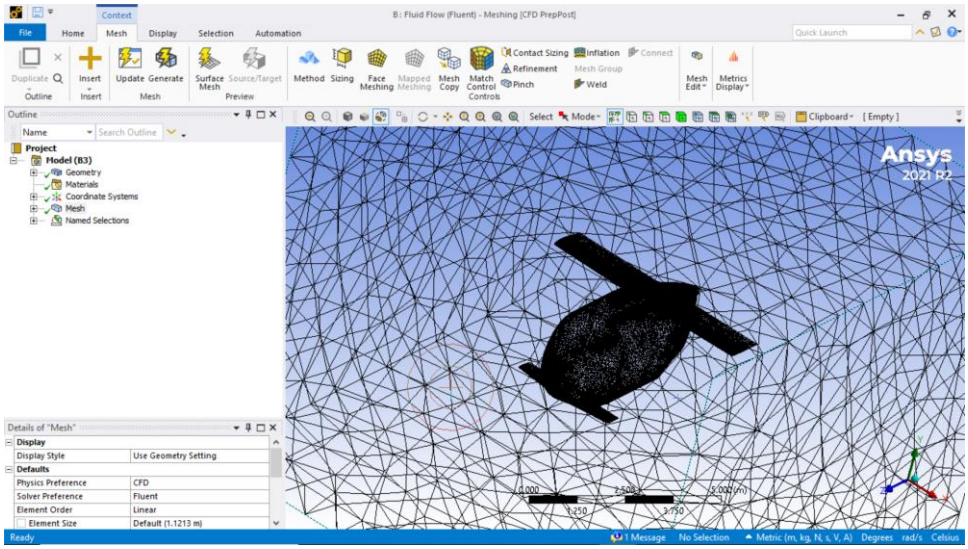

Figure 24 – Aircraft Model Mesh

2.4 Propulsion System

This section evaluates the power required by the propulsion system in each phase of the mission. The Rhacophorus has 4 EPUs (Electric Propulsion Units). These include rotor/proprotor, electric motor, and control electronics. All EPUs employ direct motor-to-propeller connection in order to eliminate the heavy gearboxes. Both EPUs in the front and rear are connected to a common gear box by a drive shaft. This was done to add redundancy to the system. In case of failure of one EPU, the motor can still be driven by the other EPU through the drive shaft.

2.5 Mission Design

The mission design from [13] is used as an inspiration and appropriated to the specifications of the *Rhacophorus*. A reserve mission is added as a contingency in case of landing failures or emergencies.

Table 3 – Mission Definition [13]

Phase		Distance [km]	Speed [m/s]	Altitude (above the highest obstacle) [m]
1	Ground Taxi (60 s)	Not applicable	2	0
2	Take-off, Hover, Transition (90)		0 to 1.2 V_{stall}	100
3	Accelerate, Climb		V for best climb rate	300
4	Cruise	100	55	300
5	Decelerate, Descend	Not applicable	V for best range	100
6	Transition, Hover (90 s)		1.2 V_{stall} to 0	0
7	Hover, Transition (90 s)		0 to 1.2 V_{stall}	100
8	Accelerate, Climb		V for best climb rate	300
9	Cruise	10	55	300
10	Decelerate, Descend		V for best range	100

11	Transition, Hover, Landing (90 s)	Not applicable	1.2 V_{stall} to 0	0
12	Ground Taxi (60 s)		2	0

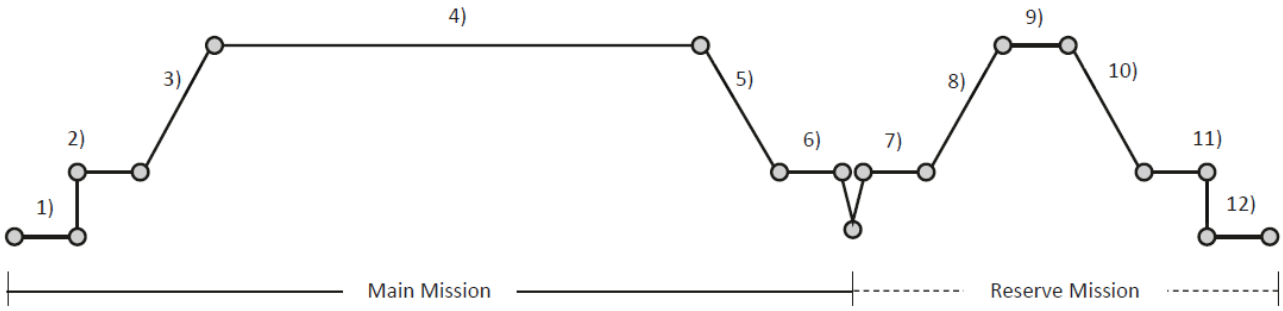

Figure 25 – Mission Definition [13]

The phase 1 is the taxying of the aircraft to the vertipad for take-off.

During phase 2, the thrust from 2 rotors and 2 proprotors of the Rhacophorus are used for lift-off and hover to prepare transition towards the climb.

Phase 3 is when the aircraft accelerates and climbs towards cruise altitude of 300 meters. The Rhacophorus employs vectored thrust from rear proprotors to add the forward thrust component.

In phase 4, the rear proprotors assume horizontal direction to propel forwards to achieve cruise at velocity about 55 m/s. Simultaneously, the wings and the front rotors produce lift to remain airborne.

Phase 5 is opposite of phase 3, the aircraft decelerates and descends to a lower altitude of 100 meters. The rear proprotors gradually assume vertical position to hover and safely descend.

Phase 6 is the reserve mission phase when the aircraft needs to abort landing and transition back to hover. In phase 7, the aircraft employs vectored to transition to a climb. Like phase 3, the phase 8 is when the aircraft accelerates and climbs back to 300 meters altitude. In phase 9, the aircraft traverses the reserve distance in cruise flight. The aircraft decelerates and descends to 100 meters altitude in phase 10. The aircraft hovers and lands in phase 11. The phase 12 is when the aircraft lands successfully and is taxied out of the vertipad.

2.6 Weight Estimation

The constituents of aircraft mass are evaluated in this section. The expression for MTOW (Maximum Take Off Mass) is as following.

$$MTOW = M_{batt} + M_{pay} + OEW \qquad \text{(Equation 6)} \quad [10]$$

Where, M_{batt} is the battery mass, M_{pay} is the mass of the payload, and OEW is the operative empty weight.

The energy required for the mission is given by the following equation.

$$E_{batt-miss} = \frac{1}{\eta_{batt}} \int_{t_{start}}^{t_{end}} P_{batt}(t)dt \qquad \text{(Equation 7)} \quad [10]$$

Where, $E_{batt-miss}$ is the total required energy by the mission, η_{batt} is the battery discharge efficiency, and $P_{batt}(t)$ is the power provided by batteries during the mission with respect to time.

3 Results and Discussion

3.1 2D Flow Over NACA2412 Airfoil

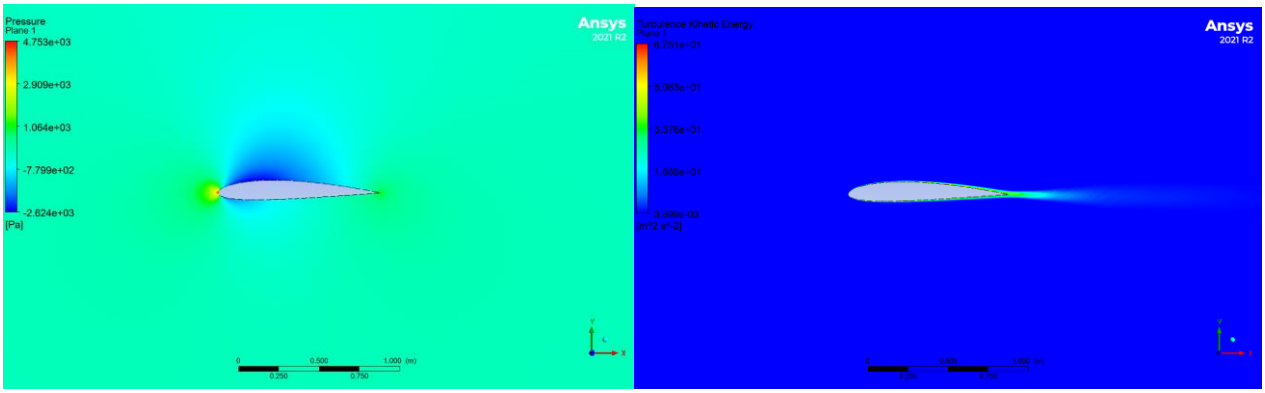

Figure 26 – Pressure (left) and turbulence (right) Contours for Flow Over NACA2412 Airfoil

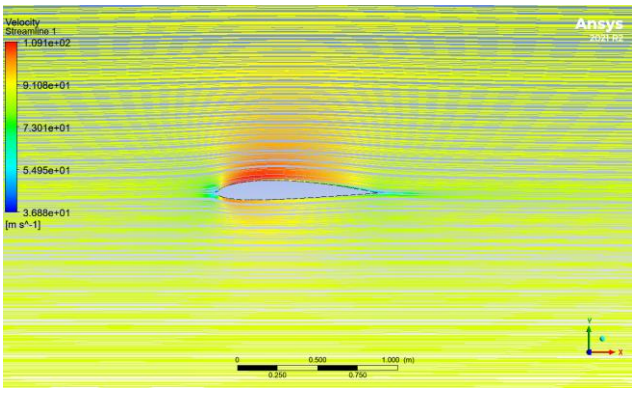

Figure 27 – Streamlines with Velocity Contour for Flow Over NACA2412 Airfoil

The pressure contour from (Figure 26) successfully demonstrates the capabilities on the airfoil. The pressure value on the suction surface is visibly lower than that of the pressure surface of the airfoil as desired. Additionally, a minimal amount was turbulence can be observed, which can be further reduced at angles of attack 4 degrees to 7 degrees. The flow separation is also very miniscule as observed in (Figure 27), therefore the risk of adverse pressure gradient minimized.

Table 4 – Variations in Coefficients of Lift and Drag at Constant Velocity 55 m/s Flow Over NACA2412.

Angle of Attack (AoA)	Coefficient of Lift (Cl)	Coefficient of Drag (Cd)	Aerodynamic Efficiency (Cl/Cd)
-2	0.005147553	0.004110168	1.25239492
-1	0.046372243	0.003822805	12.13042493
0	0.080537405	0.003750558	21.47344437
1	0.12977968	0.003855793	33.65836201
2	0.17243394	0.004210468	40.95363185
3	0.20872294	0.004636542	45.01694345
4	0.2547322	0.004938744	51.57833338
5	0.29027617	0.005575277	52.0648866
6	0.32951693	0.006381804	51.6338201
7	0.36648215	0.007057936	51.92483474
8	0.38875902	0.008971477	43.33278028
9	0.43023888	0.009386209	45.8373409
10	0. 40127684	0.014036064	28.5889862

The ratio of lift to drag force or coefficients is known as the aerodynamic efficiency of the body. This efficiency factor demonstrates the angle of attack at which the resultant aerodynamic force has a larger vertical component with respect to the horizontal component.

3.2 3D Flow Over *Rhacophorus* Fuselage and Wings

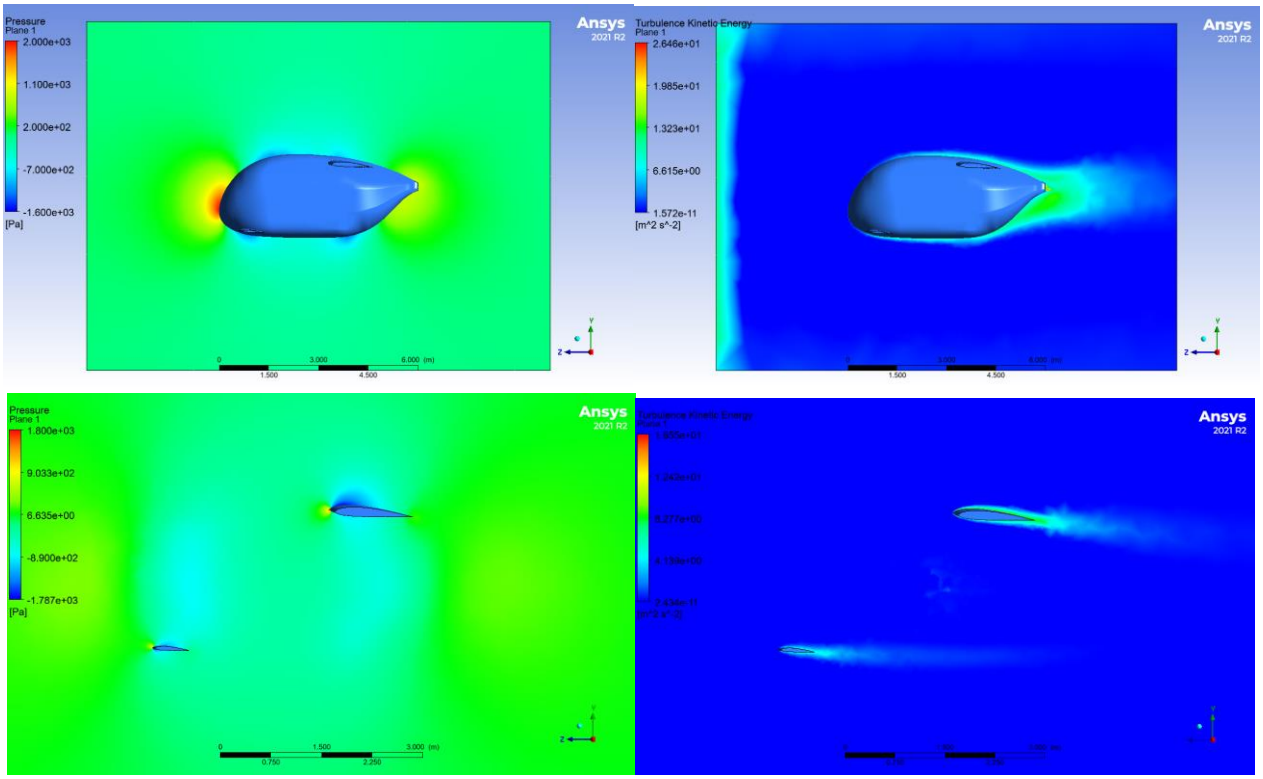

Figure 28 – Cross Section Planes of Pressure (left) and Turbulence (right) Contours for Flow Over the *Rhacophorus* Fuselage (up) and Wings (down)

The fuselage of *Rhacophorus* went through multiple iterations, refining the body shape to be more aerodynamic (Figures 13-17). The (Figure 28) shows small amount of flow separation and hence turbulence at the empennage of the fuselage and trailing edge of the wings. The small difference in the performance of the wing in 2D simulations (Figures 26,27) and 3D simulations (Figure 28) is because of the influence of flow over the fuselage to the flow over the wings. Here, it can be again noted that the pressure on the suction surface of wing is evidently lower than on the pressure surface, resulting in desired aerodynamic performance.

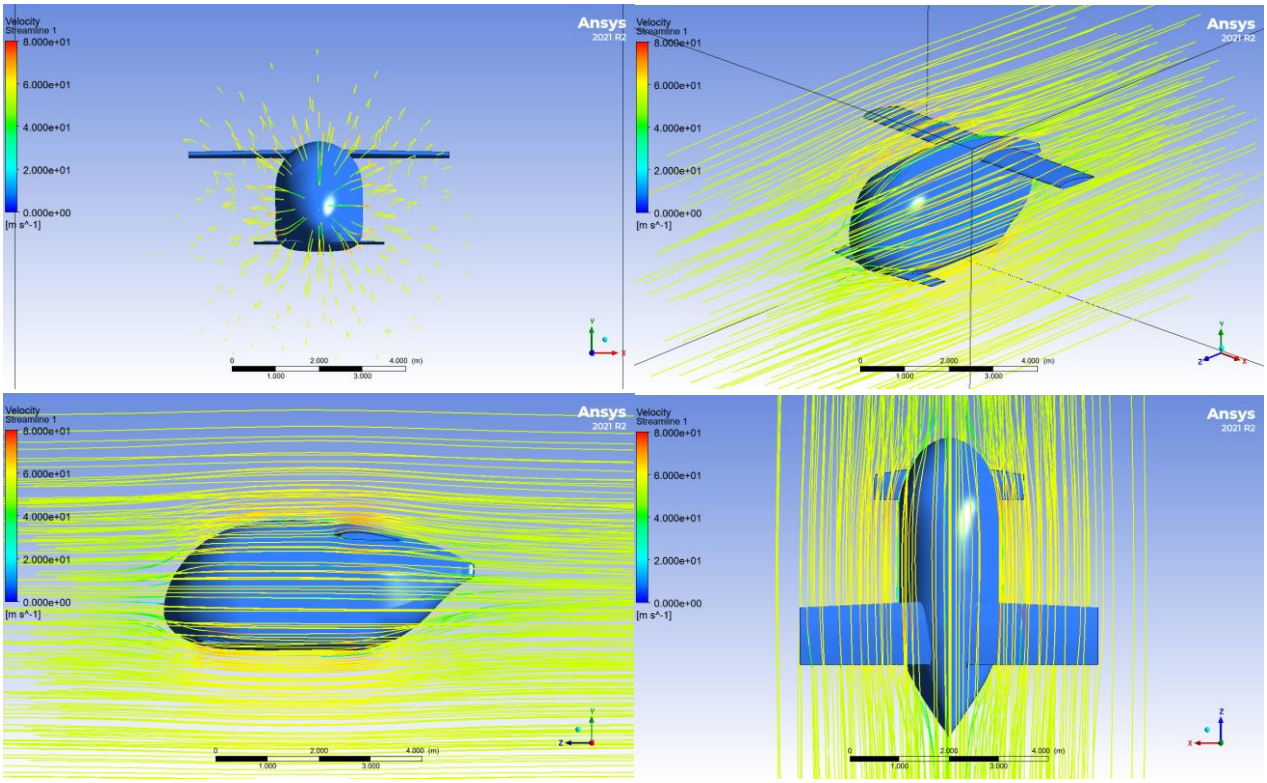

Figure 29 – Streamlines with Velocity Contour for Flow Over the *Rhacophorus*

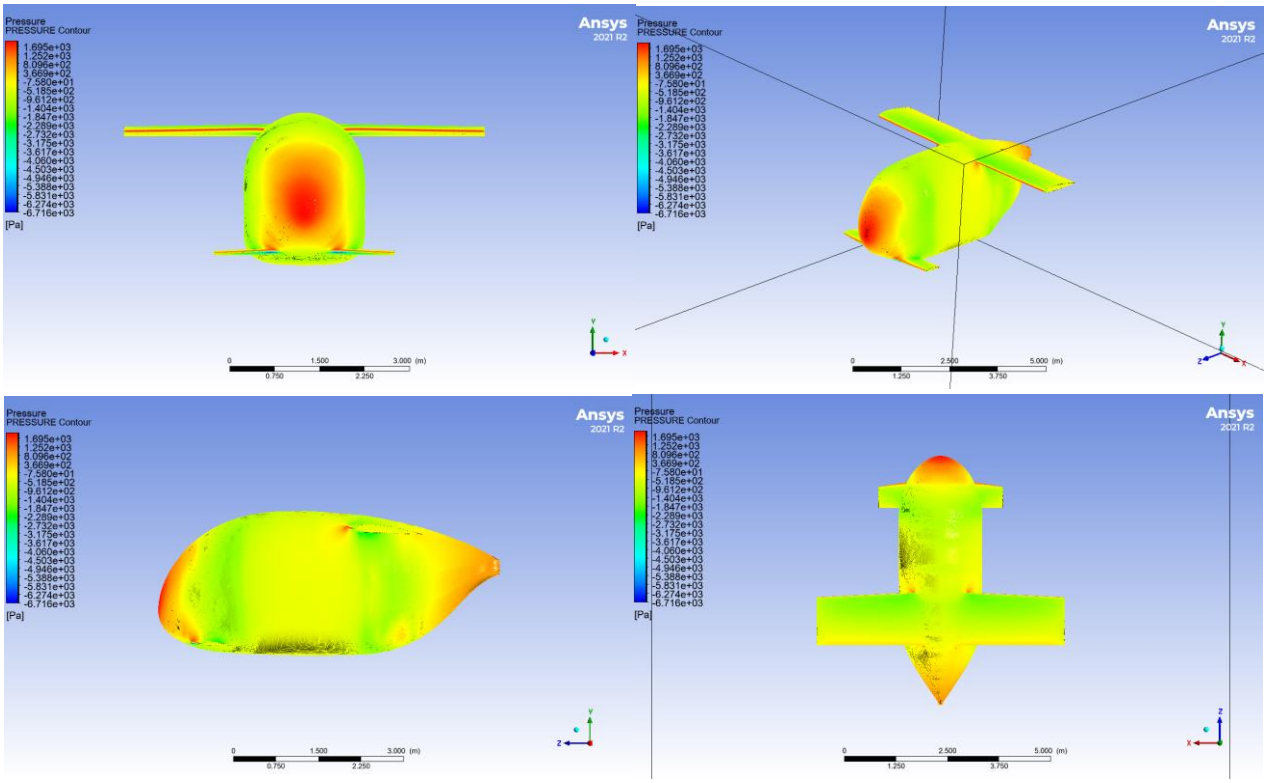

Figure 30 – Pressure Contour on the *Rhacophorus* Surface

(Figure 29) shows the flow streamlines and velocity contour in a volume surrounding the aircraft body, again this is a clearer picture of smooth streamlined flow with little to none flow reversal or adverse pressure gradient. The variation of pressure on the aircraft surface is shown in (Figure 30).

The aircraft nose and the wing leading edges have the highest pressure due to stagnation points being present at these locations. This effect could have been reduced by elongating the nose cone of the fuselage even further, however, this increased the complexities of the computer aided design, therefore further iterations were not pursued because of the time constraint. The higher pressure at the empennage is an effect of turbulent flow which is within acceptable range.

Table 5 – Simulation Results for Output Parameters Lift and Drag for the *Rhacophorus*.

Velocity [m/s]	Lift Force [N]	Drag Force [N]	Aerodynamic Efficiency (Lift/Drag)
5	23.927255	7.8157541	3.061413
10	84.843329	28.212222	3.007325
15	190.51257	60.670368	3.140126
20	339.10506	104.76375	3.236855
25	530.61318	160.13182	3.313602
30	765.11361	226.66163	3.375576
35	1042.4469	304.15422	3.427364
40	1363.0196	392.58037	3.47195
45	1726.741	491.78008	3.511206
50	2133.3069	601.65632	3.545723
55	2582.8988	722.16933	3.580093

The lift force and drag force for velocities varying from 5 m/s to 55 m/s were calculated from the simulation of flow over the aircraft, as shown in (Table 5). The aerodynamic efficiency largely remains constant, only with a slight but gradual increase with increasing velocity. This ensures consistent aerodynamic performance of the Rhacophorus throughout the mission profile (Table 3).

4 Conclusion

The Urban Air Mobility industry is yet to be market ready, but already has a plethora of innovative aircraft designs in development. Although major actors are rushing to claim early market of this industry, it must not be denied that the concept of UAM is still highly ambiguous and open ended. Therefore, a meticulous appraisal is necessary regarding the technological challenges that could constrain the industry.

The novel e-VTOL concept vehicle, Rhacophorus was designed with the help of current methodologies available in UAM development. Through numerous iterations, the design was refined until satisfactory results were visible. Since the design is only in its conceptual stage, appropriate level of design parameters were investigated. These parameters dictate if the design is ready to be passed on to preliminary design stage, where further intricacies of the design shall be investigated.

Computational Fluid Dynamics (CFD) simulations were run for the design to verify its aerodynamic performance. The results were satisfactory enough to warrant further development of the design. Some deficiencies that were apparent in the design can be corrected with further scrutiny, leaving the potential for further room for development of the project.

References

[1] Gipson, L. (2021). *UAM Vision ConOps/UAM Maturity Level 4*. [online] NASA. Available at: https://www.nasa.gov/aeroresearch/uam-vision-conops-uml-4 [Accessed 04 Sept. 2022].

[2] Tojal, M., Hesselink, H., Fransoy, A., Ventas, E., Gordo, V. and Xu, Y. (2021). Analysis of the definition of Urban Air Mobility – how its attributes impact on the development of the concept. *Transportation Research Procedia*, 59, pp.3–13. doi:10.1016/j.trpro.2021.11.091 [Accessed 04 Sept 2022].

[3] Johnson, W. (n.d.). *A Quiet Helicopter for Air Taxi Operations*. [online] Available at: https://rotorcraft.arc.nasa.gov/Publications/files/Wayne_Johnson_TVF_2020.pdf [Accessed 12 Sept. 2022].

[4] Pradeep, Priyank & Wei, Peng. (2019). Energy-Efficient Arrival with RTA Constraint for Multirotor eVTOL in Urban Air Mobility. Journal of Aerospace Information Systems. 16. 10.2514/1.I010710 [Accessed 04 Sept 2022].

[5] Volocopter. (n.d.). *Urban air mobility pioneer Volocopter*. [online] Available at: https://www.volocopter.com/urban-air-mobility/. [Accessed 27 Sept 2022]

[6] Whiteside, S., Pollard, B., Antcliff, K., Zawodny, N., Fei, X., Silva, C. and Medina, G. (2021). *Design of a Tiltwing Concept Vehicle for Urban Air Mobility*. [online] Available at: https://ntrs.nasa.gov/api/citations/20210017971/downloads/NASA-TM-20210017971.pdf [Accessed 04 Sept. 2022].

[7] Radotich, M. (n.d.). *Conceptual Design of Tiltrotor Aircraft for Urban Air Mobility*. [online] Available at: https://rotorcraft.arc.nasa.gov/Publications/files/Michael_Radotich_13-Jan-22_03-47-02.pdf [Accessed 12 Aug. 2022].

[8] www.sesarju.eu. (n.d.). *SESAR Joint Undertaking | AMU-LED - Air mobility urban - Large experimental demonstrations*. [online] Available at: https://www.sesarju.eu/projects/AMU-LED [Accessed 27 Sept. 2022].

[9] Anon, (n.d.). *AMU-LED UAM Concept of Operations – AMU-LED*. [online] Available at: https://amuledproject.eu/amu-led-uam-concept-of-operations/ [Accessed 27 Sept. 2022].

[10] Palaia, G., Abu Salem, K., Cipolla, V., Binante, V. and Zanetti, D. (2021). A Conceptual Design Methodology for e-VTOL Aircraft for Urban Air Mobility. *Applied Sciences*, 11(22), p.10815. doi:10.3390/app112210815 [Accessed 04 Sept. 2022].

[11] Bell Flight. (n.d.). *Bell-Boeing V-22 Osprey*. [online] Available at: https://www.bellflight.com/products/bell-boeing-v-22 [Accessed 25 Sept. 2022].

[12] airfoiltools.com. (n.d.). *Airfoil database search*. [online] Available at: http://airfoiltools.com/search/index [Accessed 25 Aug. 2022].

[13] Finger, D. & Götten, Falk & Braun, Carsten & Bil, Cees. (2018). Initial Sizing for a Family of Hybrid-Electric VTOL General Aviation Aircraft. 10.25967/480102 [Accessed 23 Sept. 2022].

Student Self-reflection on performance

All students must complete the following sections for every piece of work they submit using this template. The aim of this is to help you use feedback more effectively to improve your marks and your skills as a professional engineer. This section is not formally marked, but your tutor may use it when discussing your work with you.

Describe how you have used AT LEAST ONE of the following sources of information to improve this piece of work: **1.) (PREFERRED) Feedback from previous assignment(s). This can be from the same module or from a previous module or previous year of study (e.g. comments from 1st year lab formal reports should be used to help improve your 2nd year lab formal reports).** **2.) The marking criteria or rubric provided for this assignment.** **3.) The Department Technical Writing Handbook for Students.**
The department technical writing handbook proved to be especially useful resource while structuring my report.
Are there any aspects of this work that you would specifically like the marker to comment/or advise on? For example: "I wasn't sure if my figure formatting looked professional and would appreciate feedback on this aspect"
I was not sure if it was appropriate to add rough sketches of my work from before I began designing on CAD software. I would appreciate feedback on this.